ORIGINAL ARTICLE

A Graph-Based Statistical Approach to Identifying Functional Connectivity Networks in Patients with Traumatic Brain Injury

Samaneh Talebi, PhD [1]; Fatemeh Pourmotahari [2]; Keyvan Olazadeh, PhD [1, 3]; Hamid Alavi Majd, PhD [1]; Seyyed Mohammad Tabatabaei, PhD [4, 5]

[1] Department of Biostatistics, School of Allied Medical Sciences, Shahid Beheshti University of Medical Sciences, Tehran, Iran
[2] Department of Community Medicine, Dezful University of Medical Sciences, Dezful, Iran
[3] Research Center for Social Determinants of Health, Research Institute for Endocrine Sciences, Shahid Beheshti University of Medical Sciences, Tehran, Iran
[4] Department of Medical Informatics, Faculty of Medicine, Mashhad University of Medical Sciences, Mashhad, Iran
[5] Clinical Research Development Unit, Imam Reza Hospital, Faculty of Medicine, Mashhad University of Medical Sciences, Mashhad, Iran

Keywords:

Traumatic Brain Injury
Functional Magnetic Resonance Imaging
Functional Connectivity
Graph model

Received:
20-Mar-2024
Accepted:
15- May -2024
Published:
07-Jan-2025

ABSTRACT

Objectives

Traumatic brain injury (TBI) is one of the most common types of brain injuries associated with cognitive impairments. Functional magnetic resonance imaging (fMRI) studies can provide a unique opportunity to examine brain connectivity patterns and understand the neural substrates of cognitive outcomes following traumatic injury. Therefore, this study aims to determine changes in functional connectivity patterns in patients with TBI compared to healthy individuals using two graph models, adaptive dense subgraph discovery (ADSD) and variance component.

Materials & Methods

This study used fMRI data downloaded from https://openneuro.org. These data included 14 patients with TBI aged between 18 and 36 and 12 healthy individuals (female: N=6, male: N=6) aged between 19 and 52. Out of the 74 regions examined, a cluster of 18 regions related to TBI was identified using the ADSD model. Subsequently, these identified regions were used as input for the variance component model to investigate changes in connectivity patterns.

Results

Functional connectivity between an 18-brain region cluster, such as the Rectus (Left, Right), Supp_Motor_Area (Left, Right), and Middle Cingulum (Left, Right), differed between the patient and healthy groups. Based on the analysis of functional connectivity between pairs of brain regions, 153 connections between pairs of brain regions were compared in the two groups, out of which 63 connections showed significant differences between the two groups. Compared to other regions, Supp_Motor_Area_Right and Rectus_Left had more connections.

Conclusion

The study's results indicate that the functional connectivity between the Cingulum, Hippocampus, Fusiform, Supp_Motor_Area, and Precentral regions differs between the two groups. Since these regions are involved in processes such as memory, learning, spatial orientation, face recognition, coordination, and motor control, changes in their functional connectivity may lead to impairments in these areas.

How to cite this article: Talebi S, Pourmotahari F, Olazadeh K, Alavi Majd H. A Graph-Based Statistical Approach to Identifying Functional Connectivity Networks in Patients with Traumatic Brain Injury. Iran J Child Neurol. 2025; 19(1): 65-77. https://doi.org/10.22037/ijcn.v19i1.44921

*Corresponding Author: Alavi Majd H, PhD. Department of Biostatistics, School of Allied Medical Sciences, Shahid Beheshti University of Medical Sciences. Email: alavimajd@gmail.com

Introduction

Traumatic Brain Injury (TBI), also known as the silent epidemic, is one of the most significant health concerns worldwide (1). Acquired brain injuries resulting from external forces of varying intensities, ranging from mild to severe, are referred to as TBI, presenting symptoms such as decreased consciousness and alertness, memory loss, neurocognitive impairments, and even death in many cases (2, 3).

TBI is one of the most common types of brain injury that can lead to changes in the structure and function of brain networks. These changes may impact cognitive and behavioral functions (4). Brain imaging methods such as MRI and functional magnetic resonance imaging (fMRI) facilitate studying these changes, enabling the functional and structural relationships of brain networks to be examined (5).

fMRI can uncover neural activity by measuring changes in blood oxygen levels in the brain (6). Initially, this method records blood oxygen level dependent (BOLD) signals. Subsequently, the temporal correlation of these signals is estimated to examine differences in brain connectivity patterns between healthy individuals and patients (7, 8).

Based on the studies that were conducted, the networks affected by TBI include the default mode network (DMN), the executive control network (ECN), and the stimulus-driven network (SN). The DMN network is active during rest self-referential activities and personality-centered tasks. Changes in the functional connectivity (FC) of the DMN network in TBI patients can lead to cognitive impairments such as apathy (4). The ECN network is involved in cognitive control, working memory, and attention, while the SN network plays a role in detecting and responding to stimuli. Alterations in the FC of these two networks are associated with attention deficits, working memory impairments, and emotional control in TBI patients (5, 9-11).

Analyzing brain connectivity patterns using graph methods is currently one of the advanced techniques in neuroscience. In this method, the brain network is illustrated by a graph, with brain regions shown as nodes and their connections as edges. The correlations across the brain areas were calculated using these methods, and then the hypothesis of equal connectivity structure between healthy and patient groups was assessed using a statistical test (12, 13).

Estimating FC can be problematic due to the large number of correlation parameters, subject heterogeneity, and temporal autocorrelation of the data. The present study aims to examine the brain connectivity network of individuals with TBI using advanced graph theory models that address issues such as high correlation parameters and heterogeneity among individuals. The study utilizes error correction methods to control for false positives (14, 15).

Materials & Methods

Study Data

Resting-state fMRI data was downloaded from the openfmri.org repository with the accession number ds000220. 14 TBI patients (female: N=7, male: N=7, ages 18-36 years) and 12 healthy individuals (female: N=6, male: N=6, ages: 19-52 years) were examined. No significant differences were in age distribution (P-value =0.395) and gender distribution (P-value =1) between the healthy and patient groups. This study was approved by the Ethics Committee of Shahid Beheshti University of Medical Sciences (IR.SBMU.RETECH.REC.1402.433).

Data Preprocessing

The fMRI images were preprocessed using FSL software version 6.0.1. Subsequently, the preprocessed images were segmented into 90 regions of interest according to the AAL atlas using the WFU Pickatlas toolbox in MATLAB R2019b. In this study, after excluding regions with zero time series, 74 regions were examined.

Statistical Inference

Adaptive dense subgraph discovery (ADSD) and variance component models were used to compare the brain connectivity of TBI patients to the healthy group. The ADSD model is used to identify a cluster of disease-related regions, and then the variance component model is applied to compare the pairwise connectivity of the selected regions.

In the ADSD model, G = (V, E, W) represents a graph that consists of V nodes or desired regions, E = V (V-1) ⁄ 2 edges, and an adjacency matrix W. The adjacency matrix contains data regarding the edge-wise inference conclusions. G(S) = (S, E(S)) is defined as a cluster of G with S⊂V, and E(S) = {(u, v) ∈ E | u, v ∈S}. The adaptability density function is presented as follows:

$$f\ (S,\lambda) = \frac{|W(S)|}{|S|^{\lambda}} \qquad (1)$$

Where λ is used as a tuning parameter, an iterative algorithm is finally employed to optimize Eq. (1) and estimate λ.

The variance component model is defined as follows to evaluate the FC among the selected regions pairwise:

$$Y = X\beta + \varepsilon + \psi \qquad (2)$$

Where vector Y represents the correlation coefficient between the selected regions, as obtained by the ADSD model. Let X be the design matrix, and β indicates the estimation of edge parameters. The error terms ε and ψ capture the variation between edges and the subject heterogeneity, respectively.

The permutation approach employs the following test statistics to compare the FC of regions between the patient and healthy groups:

$$\left(C(\widehat{\beta_1} - \widehat{\beta_2})\right)' \left(C\left(\widehat{\mathrm{var}}(\widehat{\beta_1}) + \widehat{\mathrm{var}}(\widehat{\beta_2})\right)C'\right)^{-1} \left(C(\widehat{\beta_1} - \widehat{\beta_2})\right) \qquad (3)$$

Where C is an identity matrix. The vectors $\widehat{\boldsymbol{\beta_1}}$ and $\widehat{\boldsymbol{\beta_2}}$ represent estimates of each group's edge parameters. The false discovery rate (FDR) is used to correct multiple comparisons and adjust the p-values in Eq. (3).

FDR controls the number of false positives in tests with significant results (16). The current study examined the results using 5000 permutations. Data analysis was done using R software version 4.0.5 and MATLAB R2019b.

Results

The ADSD model was initially applied to the 74 regions extracted based on the AAL atlas. A cluster of 18 regions displayed a difference in FC between the patient and healthy groups. The regions of this cluster include Precentral_R, Supp_Motor_Area (left, right), Olfactory_L, Rectus (left, right), Cingulum_Mid (left, right), Cingulum_Post_R, Hippocampus_R, ParaHippocampal (left, right), Fusiform_R, Postcentral_L, SupraMarginal_L, Thalamus_L, Temporal_Pole_Mid_R, and Temporal_Inf_R. Figure 1 displays a cluster of brain network regions where their FC differs between the patient and healthy groups. In this figure, regions related to the disease are depicted in yellow, while other areas are depicted in red.

Figure 2 displays the -log (p-value) of pairwise FC comparisons of the 74 regions between the two groups. Regions in the plot are arranged according to the clusters identified in the ADSD model. According to this plot, regions within the cluster had higher -log (p-value), indicating that the ADSD model clustered them correctly.

Subsequently, the Component Variance model was used to compare the FC between the patient and healthy groups in the cluster. Figure 3 depicts the average correlation between all subjects in each group. Correlation values affect the circle's size and color.

Figure 4 displays the analysis results for each

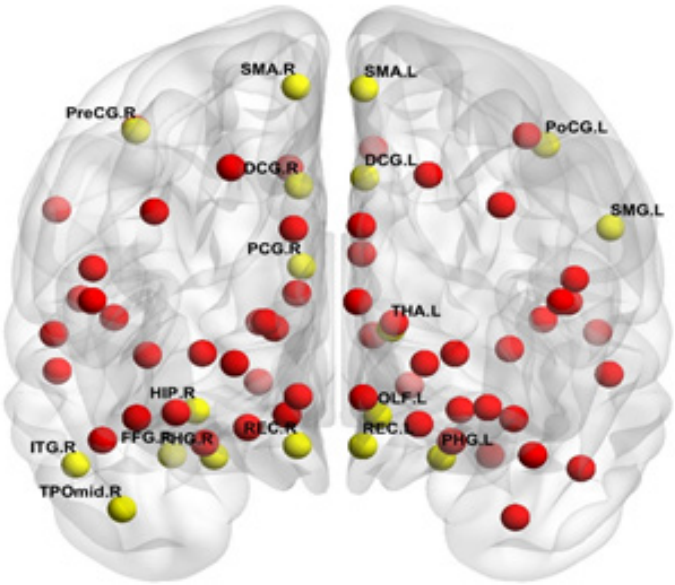

Figure 1. Disease-related regions (yellow circles) extraction by the adaptive dense subgraph discovery model

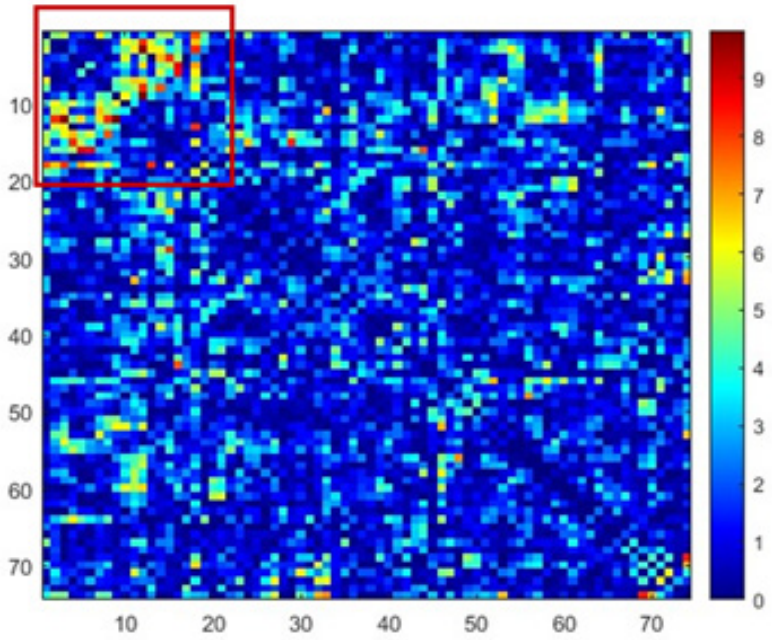

Figure 2. The –log (p - values) of the pairwise functional connectivity comparisons of 74 regions between the two groups (The cluster extraction by the adaptive dense subgraph discovery model is shown in the red box)

region's pair. There were significant differences between the two groups on 63 edges out of 18(18-1)/2 = 153.

This figure depicts the percentage difference in the correlation strengths of the regions between the two groups, with the adjusted p-values presented in the upper triangle using the FDR method.

The regions Supp_Motor_Area_R and Rectus_L had more communication than the other regions in the cluster. Significant differences were observed between the groups, with the most notable differences being -0.442, -0.410, -0.39, and -0.328, respectively. The corresponding differences were between DCG.L and PHG.R, PHG.R and SMA.L, HIP.R, and SMA.L, and PHG.R and PCG.R. Table 1 provides further details of the test results for the 63 edges, including the estimated correlation between regions in both groups and their p-values.

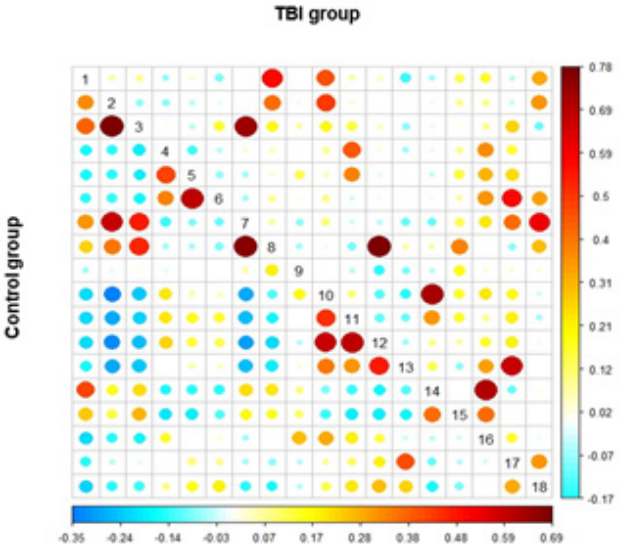

Figure 3. The average correlation of all subjects within the two groups. TBI: Traumatic Brain Injury

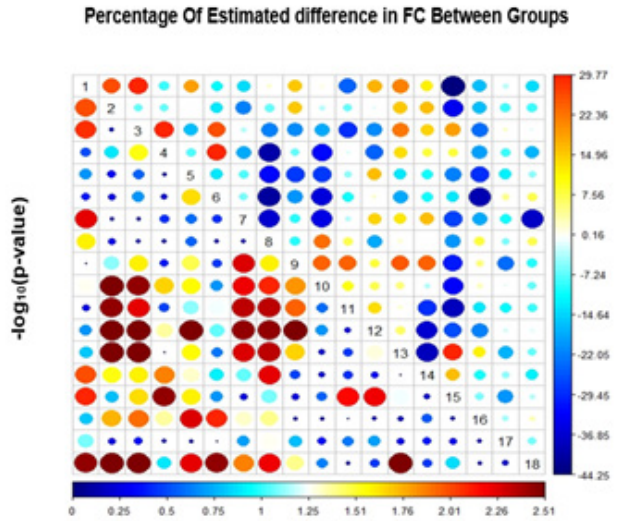

Figure 4. The results of the functional connectivity analysis for each region pair between the two groups using the variance component model. The upper-right triangle represents the difference between the two groups, and the lower-left triangle shows the amount of p-value adjusted by the FDR method

Table 1. Differentially expressed edges between the two groups by the variance component model

Index	Different expressed edges			*P*	Estimated difference*
1	PreCG.R	⟺	SMA.L	0.009	0.261
2	PreCG.R	⟺	SMA.R	0.008	0.292
3	PreCG.R	⟺	DCG.L	0.005	0.293
4	PreCG.R	⟺	DCG.R	0.025	0.189
5	PreCG.R	⟺	PoCG.L	0.009	0.258
6	PreCG.R	⟺	SMG.L	0.008	0.297
7	PreCG.R	⟺	ITG.R	0.003	-0.214
8	SMA.L	⟺	HIP.R	0.003	-0.399
9	SMA.L	⟺	PHG.L	0.003	-0.324
10	SMA.L	⟺	PHG.R	0.003	-0.410
11	SMA.L	⟺	FFG.R	0.003	-0.368
12	SMA.L	⟺	PoCG.L	0.029	0.157
13	SMA.L	⟺	THA.L	0.017	-0.211
14	SMA.L	⟺	ITG.R	0.003	-0.275
15	SMA.R	⟺	OLF.L	0.028	-0.203
16	SMA.R	⟺	PCG.R	0.025	-0.178
17	SMA.R	⟺	HIP.R	0.003	-0.327
18	SMA.R	⟺	PHG.L	0.005	-0.281
19	SMA.R	⟺	PHG.R	0.003	-0.358
20	SMA.R	⟺	FFG.R	0.003	-0.352
21	SMA.R	⟺	PoCG.L	0.025	0.238
22	SMA.R	⟺	SMG.L	0.022	0.246
23	SMA.R	⟺	THA.L	0.011	-0.240
24	SMA.R	⟺	ITG.R	0.003	-0.283
25	OLF.L	⟺	HIP.R	0.021	0.242
26	OLF.L	⟺	PHG.R	0.044	0.175
27	OLF.L	⟺	PoCG.L	0.013	-0.205
28	OLF.L	⟺	SMG.L	0.003	-0.240
29	OLF.L	⟺	THA.L	0.043	0.166
30	REC.L	⟺	REC.R	0.022	-0.182
31	REC.L	⟺	PCG.R	0.033	0.136
32	REC.L	⟺	HIP.R	0.027	0.220
33	REC.L	⟺	PHG.R	0.003	0.226
34	REC.L	⟺	FFG.R	0.027	0.135

Continued Table 1.

35	REC.L	⟺	PoCG.L	0.047	-0.132
36	REC.L	⟺	SMG.L	0.025	-0.179
37	REC.L	⟺	THA.L	0.005	0.130
38	REC.L	⟺	ITG.R	0.005	0.250
39	REC.R	⟺	THA.L	0.008	0.161
40	REC.R	⟺	ITG.R	0.003	0.244
41	DCG.L	⟺	PCG.R	0.005	-0.286
42	DCG.L	⟺	HIP.R	0.006	-0.371
43	DCG.L	⟺	PHG.L	0.004	-0.387
44	DCG.L	⟺	PHG.R	0.003	-0.442
45	DCG.L	⟺	FFG.R	0.005	-0.344
46	DCG.L	⟺	THA.L	0.047	-0.217
47	DCG.L	⟺	ITG.R	0.013	-0.272
48	DCG.R	⟺	PCG.R	0.025	-0.197
49	DCG.R	⟺	HIP.R	0.008	-0.304
50	DCG.R	⟺	PHG.L	0.004	-0.330
51	DCG.R	⟺	PHG.R	0.003	-0.387
52	DCG.R	⟺	FFG.R	0.004	-0.261
53	DCG.R	⟺	PoCG.L	0.005	0.296
54	DCG.R	⟺	THA.L	0.039	-0.167
55	DCG.R	⟺	ITG.R	0.006	-0.235
56	PCG.R	⟺	HIP.R	0.015	-0.193
57	PCG.R	⟺	PHG.L	0.011	-0.287
58	PCG.R	⟺	PHG.R	0.003	-0.392
59	PCG.R	⟺	FFG.R	0.020	-0.181
60	PCG.R	⟺	ITG.R	0.039	-0.216
61	PHG.L	⟺	SMG.L	0.006	-0.234
62	PHG.R	⟺	SMG.L	0.006	-0.194
63	FFG.R	⟺	ITG.R	0.003	-0.380

* Estimated difference of the correlation between regions in patient and healthy individuals.
Further details on the full names of the regions are available in the appendix.
Parameter estimation of the edges between regions in patient and healthy group.

Discussion

The present research utilized advanced graph theory models to analyze the brain connectivity network in individuals who have experienced TBI.

The main objective of this study was to identify a cluster of brain regions with different functional connections between the group with brain injury and the healthy group. To evaluate the FC between patients and healthy individuals, this study analyzed 74 regions. After the analysis with the ADSD model, a cluster of 18 regions showed

variations in functional connections between the two groups.

Precentral_R, Supp_Motor_Area_L, Supp_Motor_Area_R, Olfactory_L, Rectus_L, Rectus_R, Cingulum_Mid_R, Cingulum_Post_R, Hippocampus_R, ParaHippocampal_L, ParaHippocampal_R, Fusiform_R, Postcentral_L, SupraMarginal_L, Thalamus_L, Temporal_Pole_Mid_R, and Temporal_Inf_R were associated with the disease using the ADSD model. For example, the Precentral Right region of the brain refers to an area of the motor cortex located in the right part of the brain. This brain region controls various body movements, especially left-side movements. Thus, damage to this region may have serious consequences for controlling left-side movements (17).

The supplementary motor area (SMA) is a region located at the anterior edge of the brain and plays a crucial role in controlling voluntary movements and coordinating complex movements. Planned and coordinated movements are the primary functions of the SMA in the brain. The SMA is also involved in planning rapid movements. It includes coordination between different brain hemispheres and learning new movements (18).

Regions related to olfaction include the olfactory bulb and the olfactory cortex. The olfactory bulb, located near the nasal area, processes initial olfactory information, while the olfactory cortex, in the frontal and temporal lobes, processes olfactory information (19).

The Cingulum region in the brain refers to two parts: Cingulum_Mid_R (Cingulum Middle Right) and Cingulum_Mid_L (Cingulum Middle Left), located in both brain hemispheres. The Cingulum plays a role in memory and learning processes, emotional information transmission, and motor control. Cingulum_Post_R refers to the Cingulum Posterior Right, a region of the Cingulum in the brain's right hemisphere. This region is located in the brain's posterior part and posterior edge. Overall, the Cingulum Posterior plays a role in memory and emotion functions (20).

The Hippocampus, located in the medial temporal lobe, plays a crucial role in memory, learning, and spatial navigation. The Parahippocampal Gyrus is a brain region in the middle temporal lobe adjacent to the Hippocampus. It stores and retrieves spatial and visual information and performs cognitive functions (21, 22).

The Fusiform gyrus can be found in the posterior part of the temporal lobe in both hemispheres of the brain. The Fusiform Right is specifically involved in recognizing and processing visual features such as face recognition and language processing (23). Thus, depending on the severity and location of the injury, TBI can have wide-ranging effects on FC (24).

Recent studies have explored the increase or decrease in FC in patients with moderate to severe TBI compared to healthy individuals. Iraji et al. in 2016 followed 16 patients with moderate brain injury for four to six weeks post-injury. During this period, these individuals underwent fMRI neuroimaging. Additionally, 24 individuals were included as the control group. This study's results showed that patients with moderate brain injury had higher FC than the control group. The study by Iraji et al. demonstrated that the brains of individuals with moderate brain injury tend to be hyperactive to address the pathophysiological disturbances resulting from the injury. This brain response to the inflicted brain injury leads to an increase in functional connections to compensate for the damage caused by the brain trauma (25). The study results align primarily with the study

by Iraji et al., as a cluster comprising 18 brain regions in the group with brain injury showed differences in functional connections compared to the healthy group.

In 2019, Konstantinou et al. investigated the correlation between brain regions in two groups: individuals with TBI and healthy individuals. Eleven participants were in each group. The results of this study indicated that individuals with TBI had different functional connections compared to the healthy group, impacting executive functions, verbal memory, and visual memory, leading to cognitive impairments. These impairments were related to differences in FC in subcortical brain regions (26). The present study showed differences in functional connections between the TBI and healthy groups. Although this study and the study conducted by Konstantinou et al. used statistical methods to demonstrate these differences, this research employed more advanced statistical models that considered specific features of fMRI data to illustrate these differences in functional connections.

In 2020, Liyan et al. employed resting-state fMRI to study 53 brain-injured subjects and 37 healthy individuals. According to this study, FC in the brain injury group differed from the control group. Liyan et al. proposed an insight into the neurophysiological mechanisms of cognitive impairment in individuals with brain injury compared to healthy individuals (27). Their study was a cross-sectional study and utilized prevalent statistical methods such as Pearson correlation coefficient testing. This study used more appropriate statistical models to analyze fMRI neuroimaging data, which helped us to compare FC differences between the two groups more accurately. Both studies showed that functional connections in the brain injury group differed from those in the control group. However, this study examined a more significant number of brain regions. Additionally, this research discovered more diverse patterns and connections upon investigating additional areas.

Amir et al. in 2021 used the fMRI neuroimaging technique and examined functional communication among 27 patients with brain injuries and 26 normal individuals. Results revealed that FC was different in patients with brain damage compared to the control group. Amir et al. noted that this acute increase in FC may be due to the protection mechanisms after injury, a form of neurodegenerative compensation in the brain system. Amir et al.'s study also showed that the nature of this difference in FC can depend on various factors such as age, cognitive function, before injury, or the person's nervous system (28). In the present study, the increase in FC was observed in brain regions, so the two studies have the same results.

Olazadeh et al. used the longitudinal model to analyze the variances of functional communication between persons with brain injury and healthy subjects in 2022 (29). The data used in the Olazadeh study and the present study are identical. Component variance and ADSD models were used to investigate FC differences in the current study. Results of both studies indicated that functional communication was different in TBI subjects compared to the control group. This study examined more brain regions. A cluster of 18 regions shows differences in FC in the patient group compared to the healthy group. Therefore, by incorporating more regions than Olazadeh's study, this statistical model can potentially uncover a wider range of patterns and connections. With this broader analysis, we can gain a deeper understanding of the relationships

and patterns in functional connectivity among brain regions in individuals with brain injuries.

In Conclusion

Analyzing fMRI data in people with brain injury and using the component variance and ADSD models for these data can increase statistical testing power for diagnosing brain communication patterns. Fitting these models to the fMRI data showed that FC in the TBI group was different from the control group. One point to consider is that FC differences can affect cognitive functions. However, the extent and nature of this effect need more detailed studies.

Acknowledgment

This study was approved by the Ethics Committee of Shahid Beheshti University of Medical Sciences (IR.SBMU.RETECH.REC.1402.433).

Authors' contribution

Hamid Alavi Majd: The Design of Study, Project Management, Samaneh Talebi, Fatemeh Pourmotahari, and Seyyed Mohammad Tabatabaei: Data collection and analysis, Model code programming, Samaneh Talebi and Keyvan Olazadeh: The Interpretation of The Results and Writing of the Paper, Hamid Alavi Majd, Fatemeh Pourmotahari, and Seyyed Mohammad Tabatabaei: The Interpretation of Results, Reviews and Editing of the Article. All authors reviewed the results and approved the final version of the article.

Appendix

Table 1. Target Anatomical Areas according to the AAL Atlas

Index	Regions	Abbreviations	Index	Regions	Abbreviations
1	Precentral_L	PreCG.L	38	Hippocampus_R	HIP.R
2	Precentral_R	PreCG.R	39	ParaHippocampal_L	PHG.L
3	Frontal_Sup_L	SFGdor.L	40	ParaHippocampal_R	PHG.R
4	Frontal_Sup_R	SFGdor.R	41	Amygdala_L	AMYG.L
5	Frontal_Sup_Orb_L	ORBsup.L	42	Amygdala_R	AMYG.R
6	Frontal_Sup_Orb_R	ORBsup.R	43	Calcarine_L	CAL.L
7	Frontal_Mid_L	MFG.L	44	Calcarine_R	CAL.R
8	Frontal_Mid_R	MFG.R	45	Lingual_L	LING.L
9	Frontal_Mid_Orb_L	ORBmid.L	46	Lingual_R	LING.R
10	Frontal_Mid_Orb_R	ORBmid.R	47	Fusiform_L	FFG.L
11	Frontal_Inf_Oper_L	IFGoperc.L	48	Fusiform_R	FFG.R
12	Frontal_Inf_Oper_R	IFGoperc.R	49	Postcentral_L	PoCG.L
13	Frontal_Inf_Tri_L	IFGtriang.L	50	Postcentral_R	PoCG.R
14	Frontal_Inf_Tri_R	IFGtriang.R	51	SupraMarginal_L	SMG.L

Continued Appendix Table 1.

15	Frontal_Inf_Orb_L	ORBinf.L	52	SupraMarginal_R	SMG.R
16	Frontal_Inf_Orb_R	ORBinf.R	53	Precuneus_L	PCUN.L
17	Rolandic_Oper_L	ROL.L	54	Precuneus_R	PCUN.R
18	Rolandic_Oper_R	ROL.R	55	Caudate_L	CAU.L
19	Supp_Motor_Area_L	SMA.L	56	Caudate_R	CAU.R
20	Supp_Motor_Area_R	SMA.R	57	Putamen_L	PUT.L
21	Olfactory_L	OLF.L	58	Putamen_R	PUT.R
22	Olfactory_R	OLF.R	59	Pallidum_L	PAL.L
23	Frontal_Sup_Medial_L	SFGmed.L	60	Pallidum_R	PAL.R
24	Frontal_Sup_Medial_R	SFGmed.R	61	Thalamus_L	THA.L
25	Frontal_Mid_Orb_L	ORBsupmed.L	62	Thalamus_R	THA.R
26	Frontal_Mid_Orb_R	ORBsupmed.R	63	Heschl_L	HES.L
27	Rectus_L	REC.L	64	Heschl_R	HES.R
28	Rectus_R	REC.R	65	Temporal_Sup_L	STG.L
29	Insula_L	INS.L	66	Temporal_Sup_R	STG.R
30	Insula_R	INS.R	67	Temporal_Pole_Sup_L	TPOsup.L
31	Cingulum_Ant_L	ACG.L	68	Temporal_Pole_Sup_R	TPOsup.R
32	Cingulum_Ant_R	ACG.R	69	Temporal_Mid_L	MTG.L
33	Cingulum_Mid_L	DCG.L	70	Temporal_Mid_R	MTG.R
34	Cingulum_Mid_R	DCG.R	71	Temporal_Pole_Mid_L	TPOmid.L
35	Cingulum_Post_L	PCG.L	72	Temporal_Pole_Mid_R	TPOmid.R
36	Cingulum_Post_R	PCG.R	73	Temporal_Inf_L	ITG.L
37	Hippocampus_L	HIP.L	74	Temporal_Inf_R	ITG.R

Letters L and R show the left and right of the brain region

Conflict of Interest

The authors declared no conflict of interest.

References

1. Dewan MC, Rattani A, Gupta S, Baticulon RE, Hung Y-C, Punchak M, et al. Estimating the global incidence of traumatic brain injury. Journal of neurosurgery. 2018;130(4):1080-97.
2. Dang B, Chen W, He W, Chen G. Rehabilitation treatment and progress of traumatic brain injury dysfunction. Neural plasticity. 2017;2017.

3. Martínez-Molina N, Siponkoski ST, Särkämö T. Cognitive efficacy and neural mechanisms of music-based neurological rehabilitation for traumatic brain injury. Annals of the New York Academy of Sciences. 2022;1515(1):20-32.
4. Caeyenberghs K, Verhelst H, Clemente A, Wilson PH. Mapping the functional connectome in traumatic brain injury: What can graph metrics tell us? Neuroimage. 2017;160:113-23.
5. Sharp DJ, Scott G, Leech R. Network dysfunction after traumatic brain injury. Nature Reviews Neurology. 2014;10(3):156-66.
6. Kim S-G, Bandettini PA. Principles of BOLD functional MRI. Functional Neuroradiology: Principles and Clinical Applications: Springer; 2023. p. 461-72.
7. Menon SS, Krishnamurthy K. A comparison of static and dynamic functional connectivities for identifying subjects and biological sex using intrinsic individual brain connectivity. Scientific reports. 2019;9(1):5729.
8. Mohanty R, Sethares WA, Nair VA, Prabhakaran V. Rethinking measures of functional connectivity via feature extraction. Scientific reports. 2020;10(1):1298.
9. Abdul Rahman MR, Abd Hamid AI, Noh NA, Omar H, Chai WJ, Idris Z, et al. Alteration in the functional organization of the default mode network following closed non-severe traumatic brain injury. Frontiers in Neuroscience. 2022;16:833320.
10. Raizman R, Itzhaki N, Sirkin J, Meningher I, Tsarfaty G, Keren O, et al. Decreased homotopic functional connectivity in traumatic brain injury. Cerebral Cortex. 2023;33(4):1207-16.
11. Wood RL, Worthington A. Neurobehavioral abnormalities associated with executive dysfunction after traumatic brain injury. Frontiers in behavioral neuroscience. 2017;11:195.
12. Hallquist MN, Hillary FG. Graph theory approaches to functional network organization in brain disorders: A critique for a brave new small-world. Network Neuroscience. 2018;3(1):1-26.
13. Xia Y, Li L. Matrix graph hypothesis testing and application in brain connectivity alternation detection. Statistica Sinica. 2019;29(1):303-28.
14. Fiecas M, Cribben I, Bahktiari R, Cummine J. A variance components model for statistical inference on functional connectivity networks. NeuroImage. 2017;149:256-66.
15. Wu Q, Huang X, Culbreth AJ, Waltz JA, Hong LE, Chen S. Extracting brain disease-related connectome subgraphs by adaptive dense subgraph discovery. Biometrics. 2022;78(4):1566-78.
16. Benjamini Y, Hochberg Y. Controlling the false discovery rate: a practical and powerful approach to multiple testing. Journal of the Royal statistical society: series B (Methodological). 1995;57(1):289-300.
17. Banker L, Tadi P. Neuroanatomy, precentral gyrus. 2019.
18. Ruan J, Bludau S, Palomero-Gallagher N, Caspers S, Mohlberg H, Eickhoff SB, et al. Cytoarchitecture, probability maps, and functions of the human supplementary and pre-supplementary motor areas. Brain Structure and Function. 2018;223:4169-86.
19. Zhou G, Lane G, Cooper SL, Kahnt T, Zelano C. Characterizing functional pathways of the human olfactory system. Elife. 2019;8:e47177.
20. Bubb EJ, Metzler-Baddeley C, Aggleton JP. The cingulum bundle: anatomy, function, and dysfunction. Neuroscience & Biobehavioral

Reviews. 2018;92:104-27.

21. Aminoff E, Gronau N, Bar M. The parahippocampal cortex mediates spatial and nonspatial associations. Cerebral cortex. 2007;17(7):1493-503.
22. Anand KS, Dhikav V. Hippocampus in health and disease: An overview. Annals of Indian Academy of Neurology. 2012;15(4):239.
23. Palejwala AH, O'Connor KP, Milton CK, Anderson C, Pelargos P, Briggs RG, et al. Anatomy and white matter connections of the fusiform gyrus. Scientific reports. 2020;10(1):13489.
24. Nakuci J, McGuire M, Schweser F, Poulsen D, Muldoon SF. Differential patterns of change in brain connectivity resulting from severe traumatic brain injury. Brain connectivity. 2022;12(9):799-811.
25. Iraji A, Chen H, Wiseman N, Welch RD, O'Neil BJ, Haacke EM, et al. Compensation through functional hyperconnectivity: A longitudinal connectome assessment of mild traumatic brain injury. Neural Plasticity. 2016;2016.
26. Konstantinou N, Pettemeridou E, Stamatakis EA, Seimenis I, Constantinidou F. Altered resting functional connectivity is related to cognitive outcome in males with moderate-severe traumatic brain injury. Frontiers in neurology. 2019;9:1163.
27. Lu L, Li F, Chen H, Wang P, Zhang H, Chen Y-C, et al. Functional connectivity dysfunction of insular subdivisions in cognitive impairment after acute mild traumatic brain injury. Brain imaging and behavior. 2020;14:941-8.
28. Amir J, Nair JKR, Del Carpio-O'Donovan R, Ptito A, Chen JK, Chankowsky J, et al. Atypical resting state functional connectivity in mild traumatic brain injury. Brain and behavior. 2021;11(8):e2261.
29. Olazadeh K, Borumndnia N, Habibi M, Alavi Majd H. Use of the Longitudinal Model of Variance Components to Determine Hyper-Connectivity in Patients with Severe Traumatic Brain Injury Using Rs_fMRI Data. Basic and Clinical Neuroscience.0-.